Neurobiology of Disease

Neuroprotective Effect of Apolipoprotein D against Human Coronavirus OC43-Induced Encephalitis in Mice

Sonia Do Carmo,[1]* Hélène Jacomy,[2]* Pierre J. Talbot,[2] and Eric Rassart[1]

[1]Laboratoire de Biologie Moléculaire, Département des Sciences Biologiques, and BioMed, Centre de Recherches Biomédicales, Université du Québec à Montréal, Montréal, Québec, Canada H3C 3P8, and [2]Laboratory of Neuroimmunovirology, Institut National de la Recherche Scientifique–Institut Armand-Frappier, Laval, Québec, Canada H7V 1B7

Apolipoprotein D (apoD) is a lipocalin upregulated in the nervous system after injury or pathologies such as Alzheimer's disease, Parkinson's disease, and multiple sclerosis. We previously demonstrated that apoD protects against neuropathology by controlling the level of peroxidated lipids. Here, we further investigated the biological function of apoD in a mouse model of acute encephalitis. Our results show that apoD transcript and protein are upregulated during acute encephalitis induced by the human coronavirus OC43 (HCoV-OC43) infection. The apoD upregulation coincides with glial activation, and its expression returns to normal levels when the virus is cleared, concomitantly to a resolved glial reactivity. In addition, the overexpression of human apoD in the neurons of Thy-1/ApoD transgenic mice results in a threefold increase of the number of mice surviving to HCoV-OC43 infection. This increased survival rate is correlated with an upregulated glial activation associated with a limited innate immune response (cytokines, chemokines) and T-cell infiltration into infected brains. Moreover, the protection seems to be associated with a restricted phospholipase A2 activity. These data reveal a role for apoD in the regulation of inflammation and suggest that it protects from HCoV-OC43-induced encephalitis, most likely through the phospholipase A2 signaling pathways.

Key words: apolipoprotein D; inflammation; viral encephalitis; phospholipase A2; T-cell infiltration; virus

Introduction

Apolipoprotein D (apoD) is a lipocalin widely expressed in human tissues including the CNS where it is expressed mainly in glia but also in neurons (Smith et al., 1990; Provost et al., 1991; Hu et al., 2001). ApoD expression is increased in several neuropathologies such as Alzheimer's (Terrisse et al., 1998), Parkinson's (Ordoñez et al., 2006), and Niemann-Pick's type C diseases (Yoshida et al., 1996), meningoencephalitis (Terrisse et al., 1998), and multiple sclerosis (Reindl et al., 2001) (for review, see Rassart et al., 2000; Van Dijk et al., 2006). Nevertheless, the precise role of apoD in the CNS remains unknown. Early studies suggested that apoD promotes repair. Indeed, after nervous tissue injury, its expression correlated well with removal and redistribution of lipids (Boyles et al., 1990; Terrisse et al., 1999), active myelination, and axonal outgrowth (Ong et al., 1999; Rickhag et al., 2008). Moreover, apoD favors survival on an oxidative insult by controlling the levels of peroxidated lipids (Ganfornina et al., 2008).

ApoD has been shown to bind with high affinity to arachidonic acid (AA) (Morais Cabral et al., 1995), an abundant component of neural membranes (Diau et al., 2005). The liberation of AA from membrane phospholipids by phospholipases A2 (PLA2s) is an upstream regulator of many inflammatory processes involved in neuronal damage (Farooqui et al., 1997). Because apoD seems to stabilize membrane-associated AA (Thomas et al., 2003), it could restrain inflammation by limiting free AA. ApoD was already associated with inflammation because its expression is modulated in response to lipopolysaccharide in nonneuronal cells (Do Carmo et al., 2007) and in response to interleukin-1 (IL-1), IL-6, and glucocorticoids in human breast cancer cells (Blais et al., 1994, 1995). This modulation could be related to the presence of specific binding sites on the apoD promoter (Do Carmo et al., 2002, 2007).

Human coronaviruses (HCoVs) are enveloped positive-stranded RNA viruses that primarily infect the upper respiratory tract, leading to common colds (Myint et al., 1994). Moreover, they have neuroinvasive properties in human brains (Arbour et al., 2000) and could initiate neurological disorders such as multiple sclerosis (Talbot et al., 2001, 2008; Boucher et al., 2007). We previously characterized HCoV-OC43-mediated neuropathogenesis in mice (Jacomy and Talbot, 2003; Jacomy et al., 2006). C57BL/6 mice infected by an intracerebral inoculation of HCoV-OC43 developed signs of acute encephalitis. Neurons, which are the main target of infection, underwent vacuolation and degenerated by necrosis and apoptosis. Infected regions also presented microglial activation and astrogliosis, signs of a strong inflammatory reaction.

The main objective of this study was to investigate the biological role of apoD during acute viral encephalitis in a mouse model. Here, we show that, after HCoV-OC43 infection, endogenous apoD is upregulated and mice overexpressing human apoD (H-apoD) in neurons have an increased survival rate. This increased survival was correlated with an upregulated inflammatory reaction associated with a limited T-cell infiltration into infected brains. These data revealed a role for apoD in the regulation of inflammatory reactions in the brain and suggest that apoD protects from HCoV-OC43-induced encephalitis, at least in part, through the activation of signaling pathways involving PLA2.

Materials and Methods

Mice. Human apoD transgenic mice carry a construct containing the H-apoD cDNA fused to the bovine growth hormone (BGH) polyadenylation signal under the control of three different neuron-specific promoters/enhancers. In Thy-1/ApoD mice, the H-apoD expression is controlled by the promoter, the first exon, the first intron, and the 5′ noncoding region of the second exon of the human Thy-1 gene (~3.5 kb) (gift from J. Silver, New York University Medical Center, New York, NY). In NSE/ApoD mice, the rat neuron-specific enolase (NSE) promoter (~1.8 kb) (gift from G. Sutcliffe, The Scripps Research Institute, La Jolla, CA) controls the H-apoD expression. Finally, in NFL/ApoD mice, the H-apoD/BGH fragment was inserted after the promoter in the complete human neurofilament light chain (NFL) gene (gift from J.-P. Julien, Centre Hospitalier de l'Université Laval, Québec, Québec, Canada). Thus, H-apoD is expressed in neuronal cells in all regions of the nervous system. All mice were backcrossed into C57BL/6 background for at least 10 generations. Genotyping was performed on tail biopsies as described previously (Ganfornina et al., 2008). All the experimental procedures were approved by the Animal Care and Use Committees of Université du Québec à Montréal and Institut National de la Recherche Scientifique–Institut Armand-Frappier.

Virus and inoculations. The American Type Culture Collection HCoV-OC43 strain (ATCC VR-759) was grown on the HRT-18 cell line, and virus stocks [$10^{6.5}$ tissue culture infectious dose 50 ($TCID_{50}$)/ml] were kept at $-80°C$ as previously described (Jacomy and Talbot, 2003). Mice were infected at 22 d postnatal (DPN) with intracerebral (IC) inoculation of 10 μl containing 10 $TCID_{50}$ of HCoV-OC43. Control mice received an intracerebral inoculation of 10 μl of cell culture medium. Mice were killed at different days postinfection (DPI), and brain and spinal cord were collected.

Survival curves. Litters were weaned at 21 DPN and separated by sex, maintaining strain identification. The next day, all separated litters were inoculated with virus and during anesthesia ears were punched for identification and a piece of tail sectioned for genotype analysis. Then, infected mice were observed daily up to 20 DPI to monitor survival. Forty-eight transgenic Thy-1/ApoD mice and 45 wild-type (WT) littermates as well as 32 transgenic NSE/ApoD versus 51 WT littermates and 53 transgenic NFL/ApoD versus 46 WT littermates were used to establish survival curves. Survival rate was calculated at 20 d after HCoV-OC43 inoculation.

Infectious virus assays. Five transgenic mice and 5 WT littermates for each genotype were dissected at 11 DPI for infectious virus assays. Brains were homogenized to 10% (w/v) sterile PBS and centrifuged at 4°C, 20 min at 1000 $\times$ g, and supernatants were immediately frozen at $-80°C$ and stored until assayed. The extracts were processed for the presence and quantification of infectious virus by an indirect immunocytotochemistry assay, as previously described (Jacomy and Talbot, 2003).

RNA extraction and Northern blot analysis. Total RNA was extracted from brain or spinal cord by homogenization in the Trizol reagent (Invitrogen). RNA (10 μg) was separated on 1.5% (w/v) agarose-formaldehyde gels and blotted to a nylon membrane. The membranes were hybridized with [α-^{32}P]dCTP-labeled human or mouse apoD, and mouse glyceraldehyde 3-phosphate dehydrogenase (GAPDH) cDNAs. The hybridization signal was detected with a Bio-Rad Imaging screen K,

read with a PhosphorImager, and analyzed with the QuantityOne software (Bio-Rad Molecular Imager FX; Bio-Rad Laboratories).

Protein extraction and Western blot analysis. Brain and spinal cords were homogenized in lysis buffer [50 mM Tris-HCl, pH 7.3, 150 mM NaCl, 5 mM EDTA, 0.2% (v/v) Triton X-100, and 10% (w/v) Complete protease inhibitor (Roche)]. After 30 min of incubation at 4°C, lysates were sonicated and cleared by centrifugation. Protein concentration was determined using the Bio-Rad protein assay (Bio-Rad Laboratories). Proteins (10 μg per sample) were separated on a 12% (w/v) SDS-polyacrylamide gel and transferred to polyvinylidene difluoride membranes. Membranes were incubated with the primary antibodies: human apoD mouse monoclonal antibody (2B9), 1:100,000; mouse apoD rabbit polyclonal antibody, 1:500; HCoV-OC43 nucleocapsid N protein [OC43 (N)] mouse monoclonal antibody, 1:100; glial fibrillary acidic protein (GFAP) rabbit polyclonal antibody (Cell Signaling; NEB), 1:5000; Mac-2 rat monoclonal antibody (ATCC; Cedarlane), 1:100; CD4 rat monoclonal antibody (BD Pharmingen), 1:500; GAPDH mouse monoclonal antibody (Calbiochem), 1:500,000. Binding of these primary antibodies was detected with appropriate horseradish peroxidase-conjugated secondary antibodies and visualized by chemiluminescence (ECL; GE Healthcare) and x-ray film.

Immunohistochemistry. Serial vibratome sections (40 μm) of paraformadehyde-perfused brains were subjected to immunohistochemistry as described previously (Jacomy and Talbot, 2003). Viral antigens were detected with 4-E11.3 mouse monoclonal antibody (1:1000) (Bonavia et al., 1997). Astrocytes and microglia/macrophages were identified with GFAP rabbit polyclonal antibody (1:50; Dako) and Mac-2 rat monoclonal antibody (1:100; American Type Culture Collection), respectively.

Flow cytometry. Brain cell suspensions were prepared and analyzed for CD4 and CD8 cell surface expression. Briefly, brains were ground between frosted glass slides, suspended in cold RPMI 1640, and passed through nylon mesh. Percoll (GE Healthcare) was added to a final concentration of 30% (v/v) and the homogenate was centrifuged at 1300 $\times$ g for 30 min at 4°C. The cell pellet was washed and cells counted. Antibodies (BD Pharmingen) used for immunophenotyping were FITC-conjugated rat anti-mouse CD4 and PE (phycoerythrin) anti-mouse CD8a. Isotype controls (BD Pharmingen) were included for each antibody used. Flow cytometric analyses were done with a fluorescence-activated cell sorter (FACS) scanner (FACScan; BD Biosciences), and the data were processed with the WinMDI software.

Total PLA2 activity. Brains were homogenized in cold buffer (50 mM HEPES, pH 7.4, containing 1 mM EDTA; 10 ml per g of tissue) and centrifuged at 10,000 $\times$ g for 15 min at 4°C. The supernatant was used to quantify total phospholipase activity using the cPLA2 colorimetric assay kit (Cayman Chemical) without the addition of specific PLA2 inhibitors according to the manufacturer's total PLA2 activity protocol.

Cytokine quantification. Brains from Thy-1/ApoD and WT littermate mice were dissected at 8 and 11 DPI for cytokine assays. Brains were weighed and homogenized in 10% (w/v) sterile PBS, pH 7.4, containing Halt protease inhibitor mixture (Pierce; Thermo Fisher Scientific). After homogenization, tissues were centrifuged at 4°C, 15 min at 1500 $\times$ g, and then supernatants were immediately collected and stored frozen at $-80°C$ until assayed. The extracts were processed for the presence and quantification of cytokines using SearchLight Chemiluminescent Protein Arrays and were performed by the SearchLight Sample Testing Service of Pierce Biotechnology.

Statistical analyses. Survival rates were plotted as Kaplan–Meier survival curves and were compared using the log rank (Mantel–Cox) test or Student's *t* test for the survival rate at 20 DPI. One-way ANOVA was used for histogram analyses. Statistical significance was defined as $p < 0.05$.

Results

Clinical status of mice after HCoV-OC43 infection
During the first week postinfection, mice ate and drank normally and did not lose weight. Between 8 and 9 DPI, infected mice presented ruffed fur and, 1 d later, showed humped back posture, as previously described (Jacomy and Talbot, 2003). At ~11 DPI,

mice either recovered rapidly and showed no additional symptoms of encephalitis (classified as having mild signs) or they became anorexic, inactive, dehydrated, and started to die from encephalitis (classified as having severe signs). Mice with severe signs of impairment, lethargy, or eating/drinking difficulty (80–90%) were immediately killed.

ApoD is induced in the CNS of HCoV-OC43-infected mice

To investigate whether HCoV-OC43 infection modulated apoD gene transcription, infected WT mice were killed at 7, 12, and 20 DPI, and different parts of the brain were processed for the detection of apoD gene expression. Results show that apoD transcription was increased in response to HCoV-OC43 infection (Fig. 1). The CNS regions showing the highest apoD upregulation were the cortical area (cortex) and hippocampus with a fivefold and sixfold increase in expression at 7 DPI, respectively. At this time after infection, mice did not yet show pathological symptoms of infection. ApoD expression was further increased at 12 DPI, when mice began to present morbidity and reached 11- and 13-fold induction, respectively, when compared with noninfected (control) mice. At 12 DPI, apoD gene expression reached its maximum in all CNS regions tested. Its expression was increased twofold to threefold in the medulla and olfactory bulb and sixfold in cerebellum and spinal cord. At 20 DPI, apoD transcription returned to baseline levels in mice that survived the infection (Fig. 1).

ApoD induction correlates with virus load and astrocytic and microglial activation

ApoD protein levels were closely consistent with mRNA levels and were highest in cortex and hippocampus. Maximal protein levels were also observed at 12 DPI in all CNS tissues (Fig. 2), which corresponded to the time of acute phase of the encephalitis. Increased apoD levels were also consistent with the presence of HCoV-OC43. Actively replicating HCoV-OC43 could be detected at 7 DPI as well, as seen by the additional band above the OC43 (N) band, as previously described (Jacomy and Talbot, 2003). Delayed expression of apoD protein in the cerebellum and spinal cord was also correlated with delayed HCoV-OC43 replication, in accordance to virus spread and invasion of the remote areas, located far from the initial inoculation site (Fig. 2). HCoV-OC43 and apoD increases were also concomitant with astrocyte and microglia activation as detected with antibodies against the astrocyte-specific marker GFAP and the microglia activation marker Mac-2, respectively. Indeed, ApoD, GFAP, Mac-2, and virus levels were closely regulated in all analyzed CNS regions. At 20 DPI, in those mice that survived the infection, HCoV-OC43 proteins disappeared totally and apoD, GFAP, and Mac-2 returned to baseline levels, confirming that mice had recovered from the acute infection.

Transgenic mice expressing H-apoD are more resistant to acute encephalitis

To investigate the role of apoD during viral encephalitis, three different transgenic mice overexpressing H-apoD in neurons and
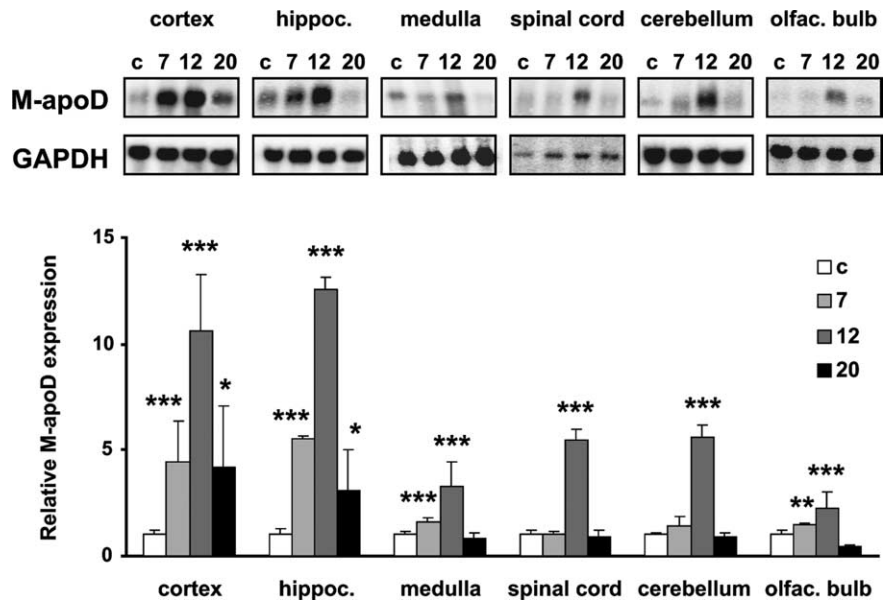

Figure 1. Effect of HCoV-OC43 infection on CNS apoD mRNA expression. Endogenous apoD expression [mouse apoD (M-apoD)] was examined by Northern blot analysis in several CNS regions of noninfected WT mice (c) and in HCoV-OC43-infected WT mice 7, 12, and 20 d postinfection. GAPDH expression was included as an internal control. Top, Representative autoradiograms. Bottom, Quantification of mRNA expression by densitometry. Values were normalized by the GAPDH expression and by the respective noninfected control, which was given an arbitrary value of 1. Values represent means ± SD ($n = 3$; performed in triplicate). $*p < 0.05$, $**p < 0.01$, $***p < 0.001$ compared with the respective noninfected control. Hippoc, Hippocampus; olfac. bulb, olfactory bulb.

WT littermates were infected by HCoV-OC43. Survival curves were established for each transgenic mouse group and compared with corresponding WT littermates (Fig. 3). Survival rates were almost three times higher in transgenic mice. Nineteen percent of the Thy-1/ApoD mice (9 mice of 48) survived after infection, whereas only 7% ($p = 0.0112$) of WT littermates (3 mice of 45) survived the infection (Fig. 3A). Moreover, males were significantly better protected by apoD overexpression, although these are more sensitive to infection. Indeed, male Thy-1/ApoD mice had a survival rate of 21% compared with 7% for WT ($p = 0.0041$) (Fig. 3B). Still, female Thy-1/ApoD mice were also less susceptible than female WT mice (Thy-1/ApoD, 16%; WT, 7%; $p = 0.0458$) (Fig. 3C). However, survival rates were similar for NSE/ApoD and NFL/ApoD compared with WT littermates, with 84% deaths for NSE/ApoD (Fig. 3D) and 79% deaths for NFL/ApoD (Fig. 3E), with no apparent difference between females and males. It is noteworthy that NSE/ApoD and NFL/ApoD mice produce moderate and low levels of H-apoD, respectively, in their CNS when compared with Thy-1/ApoD mice, in accordance with the relative strength and expression pattern of each promoter in neuronal cells (Fig. 3F). Interestingly, the NSE/apoD transgenic mice presented a survival curve that was slightly shifted in relation to time, suggesting that these mice died less rapidly from infection (Fig. 3D).

H-apoD increases infection-induced CNS glial activation

Because only Thy-1/ApoD expression seemed to confer protection against acute viral encephalitis, additional experiments were performed with these mice only. Presence of the H-apoD transgene affected neither endogenous mouse apoD mRNA expression in response to HCoV-OC43 infection (Fig. 4A) nor its protein levels (Fig. 4B). Brain infectious virus titers showed no statistical difference between Thy-1/ApoD mice and its littermates as measured at 11 DPI (Fig. 4C). Accordingly, viral nucleocapsid protein levels in the brain and spinal cord (Fig. 4B) were
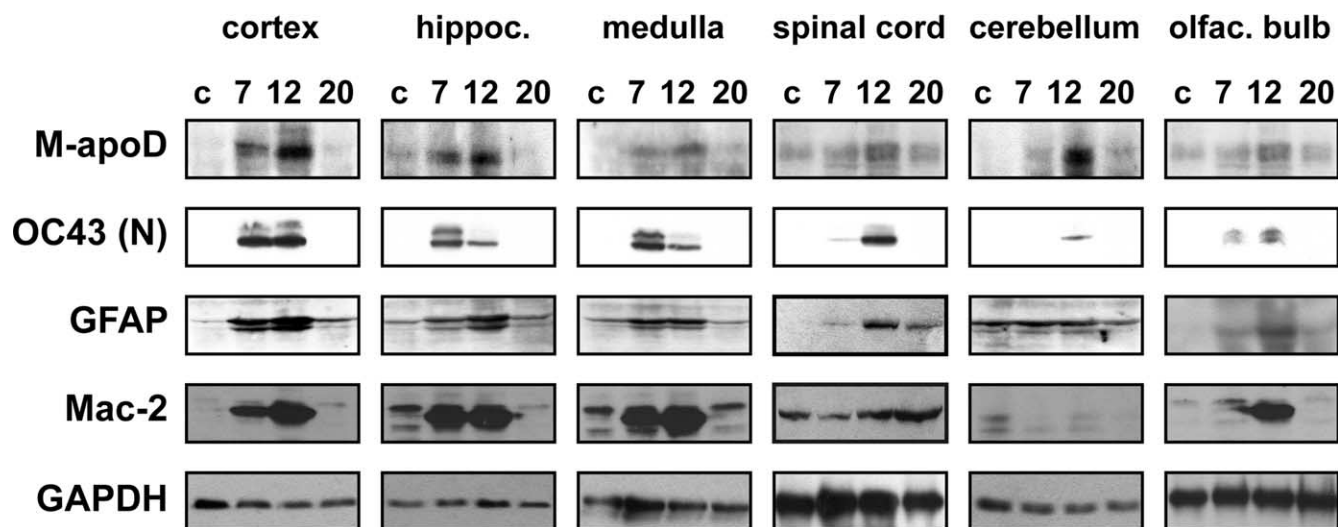
Figure 2. Western immunoblot analysis of HCoV-OC43-infected WT mice. Endogenous apoD expression [mouse apoD (M-apoD)] was examined by immunoblot in several CNS regions of noninfected control mice (c) and in HCoV-OC43-infected mice 7, 12, and 20 d postinfection. HCoV-OC43 nucleocapsid N protein [OC43 (N)], GFAP, and Mac-2 were also tested. GAPDH expression was included as an internal control. Experiments were performed in triplicate ($n = 3$). Hippoc, Hippocampus; olfac. bulb, olfactive bulb.
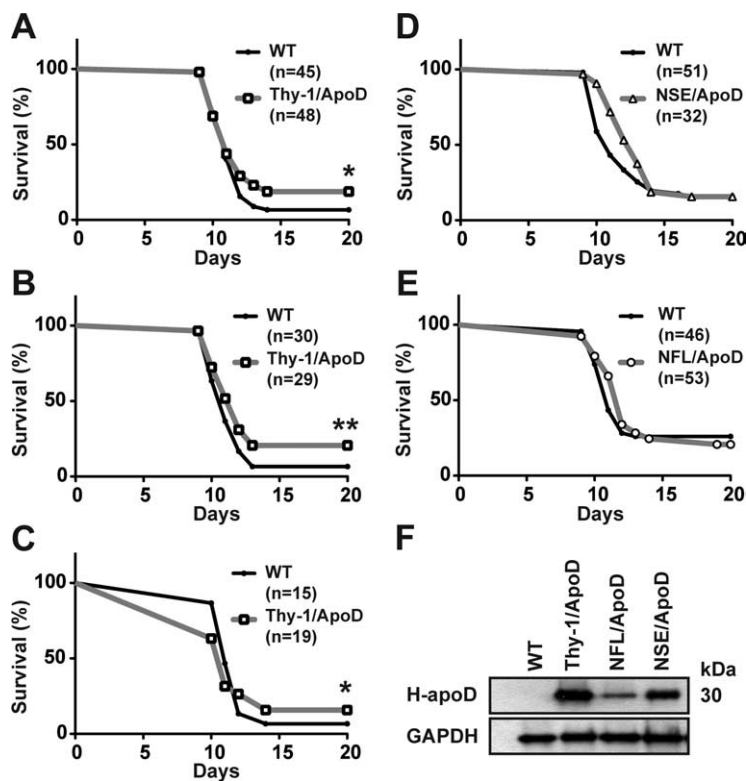

Figure 3. Survival curves of H-apoD Tg mice after HCoV-OC43 infection. Thy-1/ApoD mice present an increased survival compared with WT mice. **A–C**, This effect is observed in curves containing mixed sexes (**A**) and also when males (**B**) are analyzed separately from females (**C**). **D, E**, Survival curves of NSE/ApoD (**D**) or NFL/ApoD (**E**) mice (mixed sexes curves are presented). *$p <$ 0.05, **$p <$ 0.01 compared with corresponding WT for survival rate at 20 DPI. **F**, Immunoblot showing H-apoD protein expression in transgenic brains. GAPDH was used for normalization.

also similar in Thy-1/ApoD and in WT mice. However, astrogliosis (increased GFAP staining) and microgliosis (increased Mac-2 staining), signs of an inflammatory reaction, were observed after infection and were more evident in the CNS of Thy-1/ApoD than in WT littermates. In contrast, a decreased CD4 infiltration was evident in H-apoD-overexpressing (Thy-1/ApoD) mice compared with WT (Fig. 4B). Of note, in noninfected tissues, GFAP,

Mac-2, and CD4 levels remained similar in WT and Thy-1/apoD mice (data not shown). Immunohistochemistry on brain slices revealed a quite similar increase of activated microglial cells and astrocytes for all genotypes. Astrogliosis and microgliosis were diffused in CNS regions and found mainly in infected regions, as illustrated for hippocampus in Figure 4D. Mac-2 and GFAP staining were dependent on the region observed, the presence of virus in the region, and the intensity of the disease, mild versus severe, in WT and H-apoD mice.

Phospholipase A2 activity during infection
Total levels of PLA2 activity were measured in the brains of noninfected mice (controls) to determine baseline levels in all groups of studied mice. Quantification revealed that baseline levels were similar in WT versus transgenic mice (Fig. 5). However, after HCoV-OC43 infection, there was a 100% (twofold) increase of PLA2 activity in WT mice. In comparison, PLA2 activity in infected Thy-1/ApoD mice was also upregulated but significantly less than in infected WT mice (40%) (Fig. 5). Interestingly, NSE/ApoD and NFL/ApoD mice, which displayed the same survival curve as WT mice after infection, have levels of PLA2 activity comparable with WT mice. In addition, PLA2 activity levels were higher in NFL/ApoD than in Thy-1/ApoD mice. However, PLA2 levels in NSE/ApoD were not statistically different from those in Thy-1/ApoD mice.

H-apoD reduces T-cell infiltration into the CNS
Immunoblots already showed that CD4 was downregulated in Thy-1/ApoD compared with WT mice after HCoV-OC43 infec-

tion (Fig. 4B). To further examine T-cell infiltration, FACS analyses were conducted on total brain extracts from mice dissected at 4, 6, 8, and 11 DPI (Table 1; supplemental Fig. 1, available at www.jneurosci.org as supplemental material). In infected WT mice, both CD4- and CD8-expressing cells entered the CNS and increased significantly with time. At 11 DPI, there was a clear split between animals that will probably have survived to the infection (showing mild signs of encephalitis; 11 DPI-mild) and those that will most likely have died (showing severe signs of encephalitis; 11 DPI-severe). T-cell infiltration correlated with the outcome of the infection, because T-cell infiltration was more prominent in 11 DPI-severe than in 11 DPI-mild animals. Accordingly, a similar modulation of T-cell infiltration was observed in Thy-1/ApoD mice. Moreover, H-apoD (Thy-1/ApoD) expression in neurons significantly lowered the T-cell infiltration after infection in mice with mild as well as severe encephalitis compared with WT mice (Table 1; supplemental Fig. 1, available at www.jneurosci.org as supplemental material).

H-apoD reduces inflammatory cytokine and chemokine production

Activated microglial and astroglial cells, as well as leukocytes infiltrating the CNS, can secrete cytokines and chemokines. Therefore, we measured CNS levels of several of these proteins during the acute phase of viral encephalitis. At 8 and 11 DPI, most of inflammatory cytokines could be detected in infected brains, such as IL-1β, IL-2, IL-6, tumor necrosis factor-α (TNFα), interferon-γ (IFN-γ), or granulocyte-macrophage colony-stimulating factor (GMCSF). Although IL-1β and TNFα protein levels were similar in WT and Thy-1/ApoD mice at 8 DPI, an upregulation of IL-1β and TNFα was maintained in WT compared with Thy-1/ApoD at 11 DPI (Fig. 6A,B). In contrast, IL-6 levels were downregulated in WT versus Thy-1/ApoD mice. IL-6 acts as both a proinflammatory and antiinflammatory cytokine (Stoll et al., 2000). The role of IL-6 as an antiinflammatory cytokine role is mediated through its inhibitory effects on IL-1, and this could explain the reduction of IL1-β in Thy-1/ApoD brain. Because the matrix metalloproteinase (MMP) family members are involved in the breakdown of extracellular matrix in normal physiological processes, as well as in disease processes, we investigated the levels of MMP. Although levels of MMP-9 and MMP-3 were high in infected brains, no differences were seen between genotypes (Fig. 6C). The high levels of MMP-9 and MMP-3 could favor the traf-
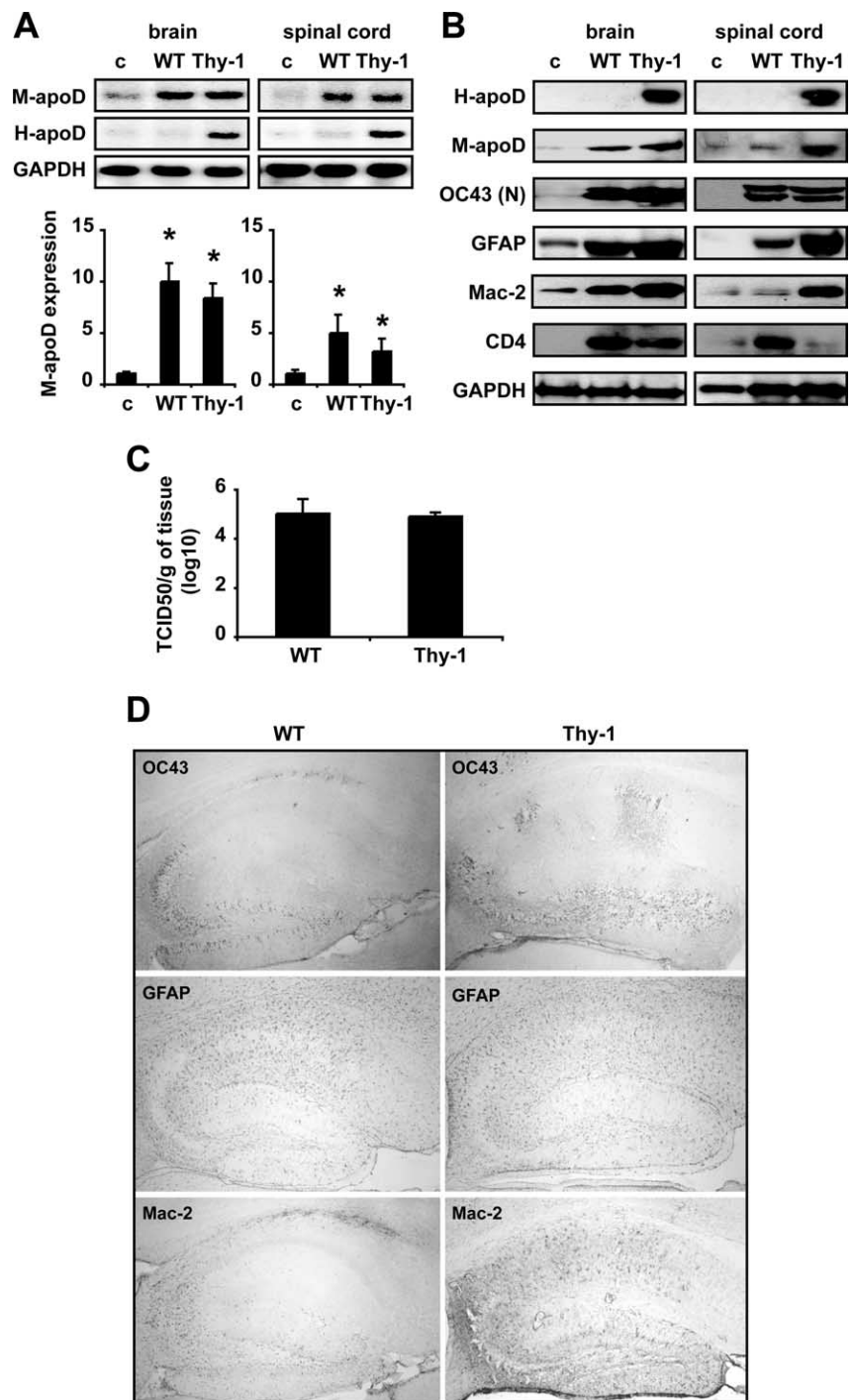

Figure 4. Analysis of Thy-1/ApoD mice 11 d after HCoV-OC43 infection. Expression levels in total brain and spinal cord of Thy-1/ApoD HCoV-OC43-infected mice are compared with noninfected (c) and infected WT mice. **A**, Northern blot analysis of mouse apoD (M-apoD). H-apoD is also presented. GAPDH was included as a loading control. M-apoD expression was quantified by densitometry. Values were normalized by the GAPDH expression and by the noninfected control. Values are means ± SD (n = 3; performed in triplicate). *p < 0.001 compared with the noninfected control. **B**, Western blot analysis of M-apoD. H-apoD, HCoV-OC43 nucleocapsid N protein [OC43 (N)], GFAP, Mac-2, and CD4 expression were also tested. GAPDH expression was included as a loading control. Experiments were performed in triplicate (n = 3). Note that the GFAP intensities for Thy-1/ApoD in brain and spinal cord are not statistically different. **C**, Amount of infectious virus detected in brain. Values are means ± SD (n = 3). **D**, Immunohistochemistry of inflammatory response in hippocampus. Astrogliosis (revealed by GFAP staining) and microgliosis (revealed by Mac-2 staining) were evident in regions in which cells are positive for viral antigens (OC43) in both WT and Thy-1/ApoD mice.

ficking of leukocytes into infected brains. We then investigated inflammatory chemokines that can modulate the recruitment of leukocytes into infected tissues. At 8 DPI, the monocyte chemoattractant protein-1 (MCP-1 or CCL2) was detected at similar

Table 1. FACS analysis of CD4$^+$ and CD8$^+$ T-cells in total brain extracts of mice at various times after intracranial inoculation with HCoV-OC43 or saline solution (control)

	Percentage of cells			
	WT		Thy-1/ApoD	
	CD4	CD8	CD4	CD8
Control	0.19 ± 0.05	0.10 ± 0.02	0.05 ± 0.02***	0 ± 0***
4 DPI	2.29 ± 0.54	1.15 ± 0.19	0.23 ± 0.08***	0.46 ± 0.14***
6 DPI	2.18 ± 0.43	3.93 ± 0.55	1.93 ± 0.43	1.95 ± 0.32***
8 DPI	2.40 ± 0.21	2.48 ± 0.46	1.31 ± 0.41***	1.31 ± 0.37***
11 DPI-mild	1.79 ± 0.98	4.60 ± 1.13	1.99 ± 0.50	2.53 ± 0.63**
11 DPI-severe	13.26 ± 2.07	6.23 ± 1.34	4.67 ± 1.98***	4.32 ± 1.69

Data represent mean values $\pm$ SD of three mice per genotype, expressed in percentage. All analyses were performed in triplicate.

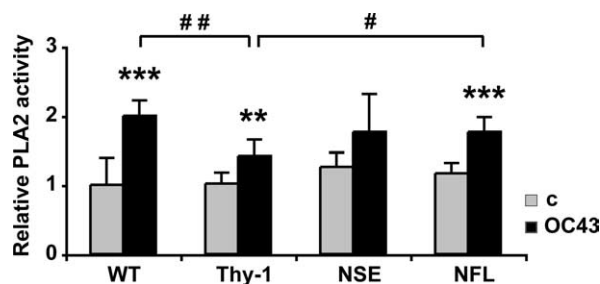**$p < 0.01$, ***$p < 0.001$ versus WT mice.

Figure 5. Total PLA2 activity. PLA2 activity was measured 11 d postinfection in HCoV-OC43 infected (OC43) and in noninfected control mice (c) and normalized by the activity in noninfected WT mice. Values are means $\pm$ SD ($n = 4$; tested in triplicate). **$p < 0.01$, ***$p < 0.001$ versus corresponding control; $^{\#}p < 0.05$, $^{\#\#}p < 0.01$.

levels in WT and Thy-1/ApoD mice. MCP-1 stimulates monocytes to leave the bloodstream, enter the surrounding tissue, and become tissue macrophages (Calvo et al., 1996). MCP-1 facilitates the migration of T-cells toward the CNS, as well (Biernacki et al., 2004). At 11 DPI, MCP-1 levels were downregulated in Thy-1/ApoD mice but remained unchanged in WT mice. At 8 DPI, T-cell-attracting [regulated on activation normal T-cell expressed and secreted (RANTES) (CCL-5) and IFN-γ-inducible protein 10 (IP-10) (CXCL-10)] chemokine levels were quite similar for both mouse genotypes (Fig. 6D). At 11 DPI, similarly to MCP-1, levels of RANTES showed a decrease in Thy-1/ApoD mice, probably resulting from a reduction of T-cell and macrophage infiltration, whereas high levels remained in WT littermates. These data are consistent with the higher T-cell infiltration observed in WT at 11 DPI (Table 1).

Discussion

Host survival to viral infections mainly depends on the ability to trigger and regulate innate and adaptive inflammatory responses, which promote clearance of virus and cell debris, as well as on its capacity to repair and/or replace damaged cells. An upregulation of apoD gene expression was previously reported in humans with meningoencephalitis (Terrisse et al., 1998) and in the CNS of mice infected by encephalitis-associated viruses such as HSV-1 (herpes simplex type-1 virus) (Kang et al., 2003), Sindbis virus (Johnston et al., 2001), JEV (Japanese encephalitis virus) (Saha and Rangarajan, 2003), or rabies virus (Prosniak et al., 2001). These observations support the hypothesis that common host cell pathways are activated in the CNS by different neurotropic and neuroinvasive viruses. Here, we report for the first time that apoD mRNA and protein are upregulated after acute viral encephalitis caused by HCoV-OC43 infection. Until now, functional upregulation of apoD during infection has remained unclear. This up-

regulation was reported in infiltrating macrophages, endothelial cells, and resident glia in SIV (simian immunodeficiency virus)-treated macaques (Roberts et al., 2003). We demonstrate that upregulation of apoD in neurons seems to confer a neuroprotective effect. Indeed, neuronal overexpression of apoD in H-apoD transgenic mice resulted in a statistically significant threefold increase in the number of mice surviving to HCoV-OC43 infection. Our results are consistent with previous reports suggesting that apoD plays a significant role in neuronal protection (Navarro et al., 1998, 2008; Franz et al., 1999; del Valle et al., 2003; Ordoñez et al., 2006; Ganfornina et al., 2008). Thus, it was proposed that neurons unable to express or to import apoD from surrounding cells are more susceptible, whereas neurons expressing apoD are more protected from degeneration (Ordoñez et al., 2006; Navarro et al., 2008).

Neuroinflammation was previously reported after infection with HCoV-OC43 (Jacomy and Talbot 2003; Butler et al., 2006; Jacomy et al., 2006). A key component of neuroinflammation is the activation of astrocytes and microglia. On activation, these cells proliferate, increase in size, change morphology, and produce cytokines. Activated microglia can also migrate to the injury site and phagocyte dead cells and cellular debris (Farooqui et al., 2007). Here, we demonstrate that, during acute encephalitis, the upregulation of endogenous apoD coincides perfectly with glial activation and that its expression returned to normal levels after clearance of the acute viral infection, concomitantly to a resolved glial reactivity.

The expression of H-apoD in neurons of Thy-1/ApoD mice, which we showed to result in an increased survival rate after acute encephalitis, was associated with an increased activation of glial cells during the acute phase of the infection. The function of activated glia in neurological disorders is a highly controversial subject. Chronic activation of glia is deleterious, in contrast to limited acute activation of glia, which is generally accepted as a beneficial response favoring organism repair. Indeed, controlled microgliosis restricts brain damage after acute brain injury probably by removing cellular debris, neurotoxic molecules, and hence providing an environment that promotes repair, neuron regeneration, and associated neuritic outgrowth (Simard and Rivest, 2007). Activated microglia can also serve as a source of trophic and growth factors (Elkabes et al., 1996). Several studies also demonstrated that astrocyte activation protects neurons by circumscribing the damaged area by the formation of a scar, by limiting leukocyte infiltration, by promoting blood–brain barrier (BBB) repair, and by sustaining neuronal survival through nutrients contribution and regulation of cell-to-cell communication (Bush et al., 1999; Faulkner et al., 2004). In other respects, it was previously reported that, after HCoV-OC43 infection, noninfected cells in close proximity to infected ones exhibited signs of apoptosis, suggesting that some inflammatory molecules, released by activated glial cells adjacent to infected neurons, are deleterious to neurons (Jacomy et al., 2006). The fact that neuronal H-apoD expression promotes both glial activation and limited leukocyte infiltration into CNS, as well as increased mouse survival to infection, suggests that apoD-induced glial activation was neuroprotective against viral damage. It has been demonstrated previously that endogenous apoD expression was increased in activated microglia cells (Gebicke-Haerter, 2005) and
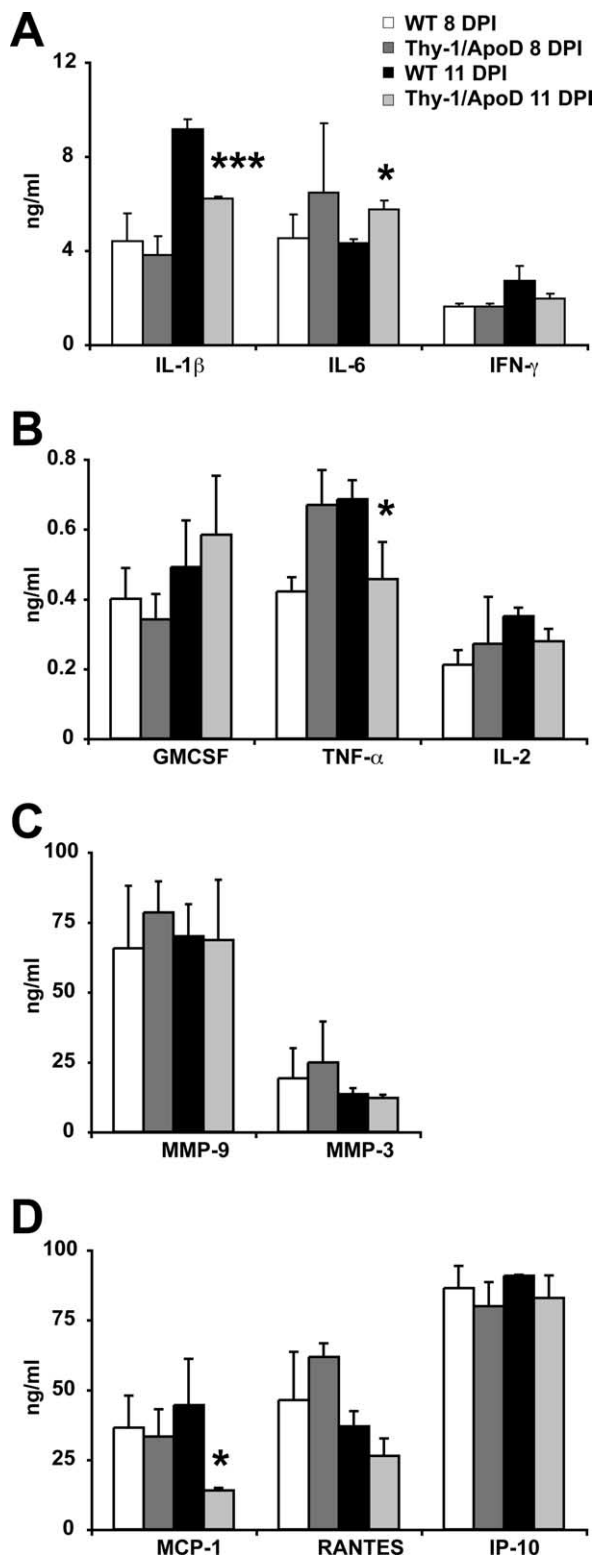
Figure 6. Innate immune response measured in brain after HCoV-OC43 infection. **A–D**, Proinflammatory cytokines (**A**, **B**), MMPs (**C**), and chemokine (**D**) protein levels were measured in WT and Thy-1/ApoD mice at 8 and 11 DPI. Values are means ± SD (8 DPI, $n = 3$; 11 DPI, $n = 2$). *$p < 0.05$, ***$p < 0.001$ versus corresponding WT.

also during inflammatory brain disorders (Franz et al., 1999; Reindl et al., 2001; Rickhag et al., 2006).

During reactive gliosis, PLA2, an important enzyme for the production of AA, is upregulated (Stephenson et al., 1996; Wal-

ton et al., 1997; Sandhya et al., 1998). The ability of specific PLA2 inhibitors to reduce neuronal damage supports an important role for AA in neurodegeneration (Farooqui et al., 2004). It was suggested previously that apoD plays an important role in the regulation of AA signaling and metabolism. ApoD could influence the availability of free AA in the cell, first by stabilizing it in cell membrane, thus preventing its liberation by PLA2; or second by binding/chelating free AA in the cytosol, thus making it unavailable for additional use in enzymatic pathways (Thomas et al., 2003). The present study suggests another way for apoD to control free AA concentration in cell: by modulating PLA2 activity. Indeed, H-apoD in Thy-1/ApoD mice prevented in part the increase of PLA2 activity after HCoV-OC43 infection. The effect on PLA2 activity is dependent on the levels of H-apoD expression. Indeed, NSE/ApoD and NFL/ApoD mice, which express lower levels of H-apoD, displayed similar levels of PLA2 activity and survival rate than WT mice after infection. The decreased PLA2 activity in Thy-1/ApoD mice is most probably related to the decreased cytokine production in these mice, because IL-1α, IL-1β, and TNFα stimulate PLA2 activity (Adibhatla and Hatcher, 2007).

It has been demonstrated previously that, after HCoV-OC43 infection, a large fraction of cells infiltrating into the CNS of the animals consists of CD4 and CD8 T-cells (Butler et al., 2006). The role played by the infiltration of inflammatory cells in HCoV-OC43 encephalitis is not well defined. Immunosuppression by cyclosporin A resulted in the acceleration of the pathology onset and increased the percentage of acute animal deaths (Jacomy and Talbot, 2003). However, HCoV-OC43-induced death is delayed in mice lacking normal B- and T-cell responses (Rag$^{-/-}$), even if, at the time of death, these mice had higher virus loads (Butler et al., 2006). These data illustrate the precarious balance between immune-mediated viral clearance and immunopathogenesis. Some chemokines are considered proinflammatory and can be induced during an immune response to recruit cells of the immune system to the site of infection. IL-1 produced by macrophages forms an important part of the inflammatory response of the body against infection (O'Neill, 2000). We demonstrated a maintained upregulation of IL-1β, particularly in WT mice at 11 DPI. This cytokine increases the expression of adhesion factors on endothelial cells to enable transmigration of leukocytes to sites of infection. Peripheral lymphocyte infiltration into the CNS was previously reported to either protect against or exacerbate encephalitic disease in CNS infection models (Stohlman et al., 1995; Irani and Griffin, 1996). We propose that an uncontrolled immune response may contribute to neuropathology, as seen in WT mice after viral encephalitis. In the same way, an increased MCP-1 was reported to contribute to virus-induced neuropathogenesis (Peterson et al., 1997; Nakajima et al., 2001). RANTES, IP-10, and MCP-1 have been previously characterized for their role in the recruitment of activated T-cells to the site of infection (Weiss et al., 1998; Babcock et al., 2003; Klein, 2004). These proinflammatory chemokines act in the development of inflammatory response and may also induce neurological damages if their synthesis is maintained. Indeed, IP-10 or MCP-1 neutralizing antibodies were shown to reduce pathology but not viral titers (Nakajima et al., 2001; Carr et al., 2003; Marques et al., 2006).

In the present study, the increased survival of Thy-1/ApoD mice correlates with a decreased number of infiltrating T-cells, associated with decreased T-cell-attracting chemokine levels (MCP-1). T-cell infiltration into CNS indicates a compromised BBB (Streit et al., 2004) and the decreased infiltration observed in transgenic mice suggests a role for apoD in BBB integrity. In

support to this, apoD is expressed in pericytes and perivascular cells in the brain (Hu et al., 2001), and it controls proliferation and migration of smooth vascular cells (Sarjeant et al., 2003; Leung et al., 2004). Furthermore, another lipocalin, the neutrophil gelatinase-associated lipocalin, is produced by the choroid plexus as a component of the innate immune response that protects the CNS from infection (Marques et al., 2008).

On top of its influence on inflammatory reactions, apoD could also positively affect the host survival by promoting CNS repair either by supporting myelination (Boyles et al., 1990; Ong et al., 1999; Terrisse et al., 1999) or by evacuating toxic metabolites such as peroxidated lipids (Ganfornina et al., 2008) or by supplying nutrients and neuroprotective factors such as estrogens and progesterone (Suzuki et al., 2007, Ghoumari et al., 2003).

A beneficial role of apoD upregulation in nervous system pathology and/or injury has often been suggested. However, although it is indeed increased in several neuropathologies, the link between apoD expression and neuronal processes remains obscure. In the present study, we demonstrate for the first time that apoD does protect from the damaging consequences of viral encephalitis, most likely by modulating inflammatory reactions. Therefore, our results, in combination with our recent study involving apoD in the defense mechanisms against oxidative stress (Ganfornina et al., 2008), suggests that apoD, as an acute phase protein, could restore the homeostatic balance after injury.

References

Adibhatla RM, Hatcher JF (2007) Secretory phospholipase A2 IIA is upregulated by TNF-alpha and IL-1alpha/beta after transient focal cerebral ischemia in rat. Brain Res 1134:199–205.

Arbour N, Day R, Newcombe J, Talbot PJ (2000) Neuroinvasion by human respiratory coronaviruses. J Virol 74:8913–8921.

Babcock AA, Kuziel WA, Rivest S, Owens T (2003) Chemokine expression by glial cells directs leukocytes to sites of axonal injury in the CNS. J Neurosci 23:7922–7930.

Biernacki K, Prat A, Blain M, Antel JP (2004) Regulation of cellular and molecular trafficking across human brain endothelial cells by Th1- and Th2-polarized lymphocytes. J Neuropathol Exp Neurol 63:223–232.

Blais Y, Sugimoto K, Carriere MC, Haagensen DE, Labrie F, Simard J (1994) Potent stimulatory effect of interleukin-1 alpha on apolipoprotein D and gross cystic disease fluid protein-15 expression in human breast-cancer cells. Int J Cancer 59:400–407.

Blais Y, Sugimoto K, Carrière MC, Haagensen DE, Labrie F, Simard J (1995) Interleukin-6 inhibits the potent stimulatory action of androgens, glucocorticoids and interleukin-1 alpha on apolipoprotein D and GCDFP-15 expression in human breast cancer cells. Int J Cancer 62:732–737.

Bonavia A, Arbour N, Yong VW, Talbot PJ (1997) Infection of primary cultures of human neural cells by human coronaviruses 229E and OC43. J Virol 71:800–806.

Boucher A, Desforges M, Duquette P, Talbot PJ (2007) Long-term human coronavirus-myelin cross-reactive T-cell clones derived from multiple sclerosis patients. Clin Immunol 123:258–267.

Boyles JK, Notterpek LM, Anderson LJ (1990) Accumulation of apolipoproteins in the regenerating and remyelinating mammalian peripheral nerve. Identification of apolipoprotein D, apolipoprotein A-IV, apolipoprotein E, and apolipoprotein A-I. J Biol Chem 265:17805–17815.

Bush TG, Puvanachandra N, Horner CH, Polito A, Ostenfeld T, Svendsen CN, Mucke L, Johnson MH, Sofroniew MV (1999) Leukocyte infiltration, neuronal degeneration, and neurite outgrowth after ablation of scar-forming, reactive astrocytes in adult transgenic mice. Neuron 23:297–308.

Butler N, Pewe L, Trandem K, Perlman S (2006) Murine encephalitis caused by HCoV-OC43, a human coronavirus with broad species specificity, is partly immune-mediated. Virology 347:410–421.

Calvo CF, Yoshimura T, Gelman M, Mallat M (1996) Production of monocyte chemotactic protein-1 by rat brain macrophages. Eur J Neurosci 8:1725–1734.

Carr DJ, Chodosh J, Ash J, Lane TE (2003) Effect of anti-CXCL10 monoclo-

nal antibody on herpes simplex virus type 1 keratitis and retinal infection. J Virol 77:10037–10046.

del Valle E, Navarro A, Astudillo A, Tolivia J (2003) Apolipoprotein D expression in human brain reactive astrocytes. J Histochem Cytochem 51:1285–1290.

Diau GY, Hsieh AT, Sarkadi-Nagy EA, Wijendran V, Nathanielsz PW, Brenna JT (2005) The influence of long chain polyunsaturate supplementation on docosahexaenoic acid and arachidonic acid in baboon neonate central nervous system. BMC Med 3:11.

Do Carmo S, Séguin D, Milne R, Rassart E (2002) Modulation of apolipoprotein D and apolipoprotein E mRNA expression by growth arrest and identification of key elements in the promoter. J Biol Chem 277:5514–5523.

Do Carmo S, Levros LC Jr, Rassart E (2007) Modulation of apolipoprotein D expression and translocation under specific stress conditions. Biochim Biophys Acta 1773:954–969.

Elkabes S, DiCicco-Bloom EM, Black IB (1996) Brain microglia/macrophages express neurotrophins that selectively regulate microglial proliferation and function. J Neurosci 16:2508–2521.

Farooqui AA, Yang HC, Horrocks L (1997) Involvement of phospholipase A2 in neurodegeneration. Neurochem Int 30:517–522.

Farooqui AA, Ong WY, Horrocks LA (2004) Biochemical aspects of neurodegeneration in human brain: involvement of neural membrane phospholipids and phospholipases A2. Neurochem Res 29:1961–1977.

Farooqui AA, Horrocks LA, Farooqui T (2007) Modulation of inflammation in brain: a matter of fat. J Neurochem 101:577–599.

Faulkner JR, Herrmann JE, Woo MJ, Tansey KE, Doan NB, Sofroniew MV (2004) Reactive astrocytes protect tissue and preserve function after spinal cord injury. J Neurosci 24:2143–2155.

Franz G, Reindl M, Patel SC, Beer R, Unterrichter I, Berger T, Schmutzhard E, Poewe W, Kampfl A (1999) Increased expression of apolipoprotein D following experimental traumatic brain injury. J Neurochem 73:1615–1625.

Ganfornina MD, Do Carmo S, Lora JM, Torres-Schumann S, Vogel M, Allhorn M, González C, Bastiani MJ, Rassart E, Sanchez D (2008) Apolipoprotein D is involved in the mechanisms regulating protection from oxidative stress. Aging Cell 7:506–515.

Gebicke-Haerter PJ (2005) Microarrays and expression profiling in microglia research and in inflammatory brain disorders. J Neurosci Res 81:327–341.

Ghoumari AM, Ibanez C, El-Etr M, Leclerc P, Eychenne B, O'Malley BW, Baulieu EE, Schumacher M (2003) Progesterone and its metabolites increase myelin basic protein expression in organotypic slice cultures of rat cerebellum. J Neurochem 86:848–859.

Hu CY, Ong WY, Sundaram RK, Chan C, Patel SC (2001) Immunocytochemical localization of apolipoprotein D in oligodendrocyte precursor-like cells, perivascular cells, and pericytes in the human cerebral cortex. J Neurocytol 30:209–218.

Irani DN, Griffin DE (1996) Regulation of lymphocyte homing into the brain during viral encephalitis at various stages of infection. J Immunol 156:3850–3857.

Jacomy H, Talbot PJ (2003) Vacuolating encephalitis in mice infected by human coronavirus OC43. Virology 315:20–33.

Jacomy H, Fragoso G, Almazan G, Mushynski WE, Talbot PJ (2006) Human coronavirus OC43 infection induces chronic encephalitis leading to disabilities in BALB/C mice. Virology 349:335–346.

Johnston C, Jiang W, Chu T, Levine B (2001) Identification of genes involved in the host response to neurovirulent alphavirus infection. J Virol 75:10431–10445.

Kang S, Seo S, Hill J, Kwon B, Lee H, Cho H, Vinay D, Kwon B (2003) Changes in gene expression in latent HSV-1-infected rabbit trigeminal ganglia following epinephrine iontophoresis. Curr Eye Res 26:225–259.

Klein RS (2004) Regulation of neuroinflammation: the role of CXCL10 in lymphocyte infiltration during autoimmune encephalomyelitis. J Cell Biochem 92:213–222.

Leung WC, Lawrie A, Demaries S, Massaeli H, Burry A, Yablonsky S, Sarjeant JM, Fera E, Rassart E, Pickering JG, Rabinovitch M (2004) Apolipoprotein D and platelet-derived growth factor-BB synergism mediates vascular smooth muscle cell migration. Circ Res 95:179–186.

Marques CP, Hu S, Sheng W, Lokensgard JR (2006) Microglial cells initiate vigorous yet non-protective immune responses during HSV-1 brain infection. Virus Res 121:1–10.

Marques F, Rodrigues AJ, Sousa JC, Coppola G, Geschwind DH, Sousa N, Correia-Neves M, Palha JA (2008) Lipocalin 2 is a choroid plexus acute-phase protein. J Cereb Blood Flow Metab 28:450–455.

Morais Cabral JH, Atkins GL, Sánchez LM, López-Boado YS, López-Otin C, Sawyer L (1995) Arachidonic acid binds to apolipoprotein D: implications for the protein's function. FEBS Lett 366:53–56.

Myint S, Johnston S, Sanderson G, Simpson H (1994) Evaluation of nested polymerase chain methods for the detection of human coronaviruses 229E and OC43. Mol Cell Probes 8:357–364.

Nakajima K, Honda S, Tohyama Y, Imai Y, Kohsaka S, Kurihara T (2001) Neurotrophin secretion from cultured microglia. J Neurosci Res 65:322–331.

Navarro A, Tolivia J, Astudillo A, del Valle E (1998) Pattern of apolipoprotein D immunoreactivity in human brain. Neurosci Lett 254:17–20.

Navarro A, Ordóñez C, Martínez E, Pérez C, Astudillo A, Tolivia J (2008) Apolipoprotein D expression absence in degenerating neurons of human central nervous system. Histol Histopathol 23:995–1001.

O'Neill L (2000) The Toll/interleukin-1 receptor domain: a molecular switch for inflammation and host defence. Biochem Soc Trans 28:557–563.

Ong WY, Lau CP, Leong SK, Kumar U, Suresh S, Patel SC (1999) Apolipoprotein D gene expression in the rat brain and light and electron microscopic immunocytochemistry of apolipoprotein D expression in the cerebellum of neonatal, immature and adult rats. Neuroscience 90:913–922.

Ordóñez C, Navarro A, Perez C, Astudillo A, Martínez E, Tolivia J (2006) Apolipoprotein D expression in substantia nigra of Parkinson disease. Histol Histopathol 21:361–366.

Peterson PK, Hu S, Salak-Johnson J, Molitor TW, Chao CC (1997) Differential production of and migratory response to beta chemokines by human microglia and astrocytes. J Infect Dis 175:478–481.

Prosniak M, Hooper DC, Dietzschold B, Koprowski H (2001) Effect of rabies virus infection on gene expression in mouse brain. Proc Natl Acad Sci U S A 98:2758–2763.

Provost PR, Villeneuve L, Weech PK, Milne RW, Marcel YL, Rassart E (1991) Localization of the major sites of rabbit apolipoprotein D gene transcription by in situ hybridization. J Lipid Res 32:1959–1970.

Rassart E, Bedirian A, Do Carmo S, Guinard O, Sirois J, Terrisse L, Milne R (2000) Apolipoprotein D. Biochim Biophys Acta 1482:185–198.

Reindl M, Knipping G, Wicher I, Dilitz E, Egg R, Deisenhammer F, Berger T (2001) Increased intrathecal production of apolipoprotein D in multiple sclerosis. J Neuroimmunol 119:327–332.

Rickhag M, Wieloch T, Gidö G, Elmér E, Krogh M, Murray J, Lohr S, Bitter H, Chin DJ, von Schack D, Shamloo M, Nikolich K (2006) Comprehensive regional and temporal gene expression profiling of the rat brain during the first 24 h after experimental stroke identifies dynamic ischemia-induced gene expression patterns, and reveals a biphasic activation of genes in surviving tissue. J Neurochem 96:14–29.

Rickhag M, Deierborg T, Patel S, Ruscher K, Wieloch T (2008) Apolipoprotein D is elevated in oligodendrocytes in the peri-infarct region after experimental stroke: influence of enriched environment. J Cereb Blood Flow Metab 28:551–562.

Roberts ES, Zandonatti MA, Watry DD, Madden LJ, Henriksen SJ, Taffe MA, Fox HS (2003) Induction of pathogenic sets of genes in macrophages and neurons in NeuroAIDS. Am J Pathol 162:2041–2057.

Saha S, Rangarajan PN (2003) Common host genes are activated in mouse brain by Japanese encephalitis and rabies viruses. J Gen Virol 84:1729–1735.

Sandhya TL, Ong WY, Horrocks LA, Farooqui AA (1998) A light and electron microscopic study of cytoplasmic phospholipase A2 and cyclooxygenase-2 in the hippocampus after kainate lesions. Brain Res 788:223–231.

Sarjeant JM, Lawrie A, Kinnear C, Yablonsky S, Leung W, Massaeli H, Prichett W, Veinot JP, Rassart E, Rabinovitch M (2003) Apolipoprotein D inhibits platelet-derived growth factor-BB-induced vascular smooth muscle cell proliferated by preventing translocation of phosphorylated extracellular signal regulated kinase 1/2 to the nucleus. Arterioscler Thromb Vasc Biol 23:2172–2177.

Simard AR, Rivest S (2007) Neuroprotective effects of resident microglia following acute brain injury. J Comp Neurol 504:716–729.

Smith KM, Lawn RM, Wilcox JN (1990) Cellular localization of apolipoprotein D and lecithin:cholesterol acyltransferase mRNA in rhesus monkey tissues by in situ hybridization. J Lipid Res 31:995–1004.

Stephenson DT, Lemere CA, Selkoe DJ, Clemens JA (1996) Cytosolic phospholipase A2 (cPLA2) immunoreactivity is elevated in Alzheimer's disease brain. Neurobiol Dis 3:51–63.

Stohlman SA, Bergmann CC, van der Veen RC, Hinton DR (1995) Mouse hepatitis virus-specific cytotoxic T lymphocytes protect from lethal infection without eliminating virus from the central nervous system. J Virol 69:684–694.

Stoll G, Jander S, Schroeter M (2000) Cytokines in CNS disorders: neurotoxicity versus neuroprotection. J Neural Transm Suppl 59:81–89.

Streit WJ, Mrak RE, Griffin WS (2004) Microglia and neuroinflammation: a pathological perspective. J Neuroinflammation 1:14.

Suzuki S, Gerhold LM, Böttner M, Rau SW, Dela Cruz C, Yang E, Zhu H, Yu J, Cashion AB, Kindy MS, Merchenthaler I, Gage FH, Wise PM (2007) Estradiol enhances neurogenesis following ischemic stroke through estrogen receptors alpha and beta. J Comp Neurol 500:1064–1075.

Talbot PJ, Arnold D, Antel JP (2001) Virus-induced autoimmune reactions in the CNS. Curr Top Microbiol Immunol 253:247–271.

Talbot PJ, Jacomy HJ, Desforges M (2008) Pathogenesis of human coronaviruses other than severe acute respiratory syndrome coronavirus. In: Nidovirus (Perlman S, Gallagher T, Snijder EJ, eds), pp 313–324. Washington, DC: ASM.

Terrisse L, Poirier J, Bertrand P, Merched A, Visvikis S, Siest G, Milne R, Rassart E (1998) Increased levels of apolipoprotein D in cerebrospinal fluid and hippocampus of Alzheimer's patients. J Neurochem 71:1643–1650.

Terrisse L, Séguin D, Bertrand P, Poirier J, Milne R, Rassart E (1999) Modulation of apolipoprotein D and apolipoprotein E expression in rat hippocampus after entorhinal cortex lesion. Brain Res Mol Brain Res 70:26–35.

Thomas EA, Copolov DL, Sutcliffe JG (2003) From pharmacotherapy to pathophysiology: emerging mechanisms of apolipoprotein D in psychiatric disorders. Curr Mol Med 3:408–418.

Van Dijk W, Do Carmo S, Rassart E, Dahlbäck B, Sodetz JM (2006) The plasma lipocalins α1-acid glycoprotein, apolipoprotein D, apolipoprotein M and complement protein C8γ. In: Lipocalins (Akerström B, Borregaard N, Flower DR, Salier JP, eds), pp 140–166. Georgetown, TX: Landes Bioscience.

Walton M, Sirimanne E, Williams C, Gluckman PD, Keelan J, Mitchell MD, Dragunow M (1997) Prostaglandin H synthase-2 and cytosolic phospholipase A2 in the hypoxic-ischemic brain: role in neuronal death or survival? Brain Res Mol Brain Res 50:165–170.

Weiss JM, Downie SA, Lyman WD, Berman JW (1998) Astrocyte-derived monocyte-chemoattractant protein-1 directs the transmigration of leukocytes across a model of the human blood-brain barrier. J Immunol 161:6896–6903.

Yoshida K, Cleaveland ES, Nagle JW, French S, Yaswen L, Ohshima T, Brady RO, Pentchev PG, Kulkarni AB (1996) Molecular cloning of the mouse apolipoprotein D gene and its upregulated expression in Niemann-Pick disease type C mouse model. DNA Cell Biol 15:873–882.